JTTEE5 19:736–744
DOI: 10.1007/s11666-010-9494-z
1059-9630/$19.00 © ASM International

Analysis of the Microstructure of Thermal Spray Coatings: A Modeling Approach

Hamideh B. Parizi, Javad Mostaghimi, Larry Pershin, and Hamid S. Jazi

(Submitted November 12, 2009; in revised form March 1, 2010)

Microstructure of coatings produced by thermal spray coating process depends on many parameters, including particle impact conditions, powder materials, and substrate conditions. Because of the large number of parameters affecting microstructure, developing a computational tool that can predict the microstructure of thermal spray coatings as a function of these parameters can be of great interest as it will save time and resources when developing new coatings. In this article, we examine the validity and the accuracy of such a computational tool. We present the result of a three-dimensional model of coating formation. The model is based on the Monte Carlo method with particle impact conditions, materials properties of powder, and substrate as input. The output of the model includes coating porosity, surface roughness, and coating thickness. In order to validate the model, coatings under specific conditions were deposited and the predicted results were compared to the actual deposits. The impact conditions for these cases were measured by DPV-2000 and the raw data were used as input to the computer program. The comparison between the actual deposits and the simulated ones shows good agreement. The results demonstrate the viability and usefulness of this modeling tool in developing new coatings and understanding their microstructure.

Keywords influence of process parameters, properties of coatings, spray deposition

1. Introduction

SimCoat (Simulent, Inc., Toronto, Canada), a software developed to model the formation of thermal spray coatings, was used to model the deposition of alumina and zirconia powders on a stainless steel surface.

The software is based on a stochastic model and predicts the average thickness, roughness, and porosity of the coating. The input to the model includes the in flight conditions of the injected powder and their physical and transport properties as well as the substrate properties. More information about the numerical modeling can be found in Ref 1-5.

The model was previously employed to study the coating properties of moving and stationary plasma torches under different spraying conditions. However, there are three major differences between the present simulations and those presented in previous articles:

1. The sizes of the substrate were usually much smaller in the previous simulations, e.g., 1 by 1 mm (Ref 4, 5). This was due to the inefficiency in the computational algorithm which made simulations on large substrates prohibitively expensive.
2. The number of passes of the moving gun were usually limited, e.g., 8 passes.
3. In the original version, particle impact conditions, i.e., particle size D, velocity V, temperature T, spray dispersion angle, and azimuthal angle, were chosen randomly from prescribed normal distributions of these parameters. User-specified mean and standard deviation for each of the above-mentioned parameters were assigned to the normal distribution of each variable. The means and standard deviations can be obtained from the measurements performed by DPV-2000 diagnostic system.

In the present work, the substrate size is substantially larger, 25 by 25 mm and 6 by 25 mm. By increasing the substrate size, the calculation time as well as the need for memory increases. The code has been optimized such that it is now possible to run the simulations for much larger substrates. Therefore, these simulations are better representations of the actual coating samples used to study microstructure.

We have increased the number of passes substantially. To be able to compare the simulation results to experiments, the total numbers of passes for alumina and zirconia coatings were 40 and 65, respectively. The increase in the number of passes would result in an increase in the number of cells perpendicular to the substrate as well as the simulation time. However, the code has been optimized in such a way that it can perform the simulations efficiently in a matter a few hours on a PC.

The original software was modified to accept the initial particles' conditions directly from the DPV2000 measurements. In the present DPV measurements, two types

Hamideh B. Parizi, Simulent, Inc., Toronto, ON, Canada; and **Javad Mostaghimi, Larry Pershin,** and **Hamid S. Jazi**, Centre for Advanced Coating Technologies, Faculty of Applied Science and Engineering, University of Toronto, Toronto, ON, Canada. Contact e-mail: mostag@mie.utoronto.ca.

of data were collected by 7 by 7 grid scans at 3 mm steps and 100 mm spray distance prior to coatings deposition. In one file, the information on all particles passing through a specific region during this time is recorded. The information includes diameter, velocity, and temperature of the in-flight particles. This information is then used to calculate the average diameter, temperature, and velocity of particles passing through a specific region, as well as the statistical information about the mean and standard deviation of velocity, diameter, and temperature during the deposition. *SimCoat* software is designed to accept both of the following options:

1. Using a normal distribution function and a random number generator, a diameter, velocity, and temperature is assigned to each particle that is incident on the substrate. The random generation routine generates these values independent of each other. It has been previously shown that this model can reasonably predict coating properties (Ref 1-5). The model, however, assumes that particle impact conditions are independent from each other. In reality, they are not completely independent and this may result in the selection of unreasonable impact conditions for some of the particles. For example, to a particle with a small diameter, a very small velocity or a very low temperature may be assigned and vice versa.
2. In order to produce more realistic results, the code has been modified to accept the raw DPV-2000 data measurements. In this case, the calculation domain (substrate) will be divided into the same size grids as the one used by DPV-2000 instrument. Then, for each particle impacting at a specific location on the substrate, the program searches the database that has been generated from the DPV measurements, finds the same region, and randomly picks the diameter of the particle and the corresponding measured temperature and velocity. This assignment of the droplet properties is more realistic and closer to the actual conditions in the coating process. For example, it is known that the core of the plasma plume is usually its hottest part. Therefore, the user will be assured that all particles used in the simulation which are located in the middle of plume are hotter than the particles close to the periphery of the plume. Since there is no random assignment of temperature and velocity, the coating properties should be better predicted.

In the present work, both methods have been used to simulate the coating of alumina and zirconia on a stainless steel substrate and the results are compared with each other and with the experimental measurements performed under the same conditions.

2. Experimental Method and Results

Experiments were carried out and coatings were deposited using an Axial III plasma torch with axial injection of powders (Northwest Mettech, North Vancouver, Canada). The spray process parameters are listed in Table 1. The torch was mounted on a robot and it was moved with a speed of approximately 64 cm/s in the horizontal direction and with a step size of 5.5 mm in the vertical direction.

Table 1 Plasma spray parameters

Gun	Axial III
Current per electrode, A	230
Voltage, V	160-175
Gas flow rate, (Nitrogen), slpm	200 (for Zirconia) 150 (for Alumina)
Feed rate, g/min	40
Spray distance, mm	100

In-flight particle conditions were measured by a DPV-2000 system (Tecnar Ltee, Montréal, QC, Canada). The variation of in-flight particle conditions through the cross section of the plasma plume was collected by 7 by 7 grid scans at 3 mm steps at 100 mm spray distance, prior to coatings deposition.

Two types of powder were used: ZrO_2 18% $TiO_2$10%Y_2O_3 powder was Metco 143 (Sulzer-Metco, Westbury, NY) with $-75+5$ μm particle size distribution. Another powder was (Al_2O_3 3% TiO_2) Metco 101NS with $-45+11$ μm. Actual particle size distributions for both powders (Fig. 1) were measured by a laser diffraction particle size analyser (Mastersizer 200, Malvern Instruments, Malvern, UK). The measurements results were used to calibrate DPV 2000.

Zirconia coating thickness was 70 μm after 13 layers of the torch with the given powder feed rate of 40 g/min; the alumina coating thickness was 170 μm after 10 layers. All coatings were deposited on a grit blasted stainless steel substrates 25 by 25 by 3 mm^3 initially at room temperature. Surface roughness of coatings was measured by a stylus profilometer (Precision Devices Inc., Michigan).

Cross sections through the deposited coatings were polished and examined under a scanning electron microscope, Hitachi-S570. Coating porosity was measured using image analysis software (Optimas6, Media Cybernetics, Silver Spring, MD). Figures 2 and 3 show cross sections of Alumina and Zirconia coatings, respectively.

3. The Model

A three-dimensional stochastic model based on the Monte Carlo method has been developed to simulate microstructure of thermal spray coatings as a function of process parameters (Ref 1-3). The coating is assumed to consist of splats deposited on each other, with voids forming between them leading to porosity. The model predicts the variation of coating porosity, thickness, and roughness with particle impact conditions and the torch trajectory and speed.

In an earlier version of the model (Ref 1-3) it was assumed that porosity formation within the coating is entirely due to the thermal stresses within the splats that

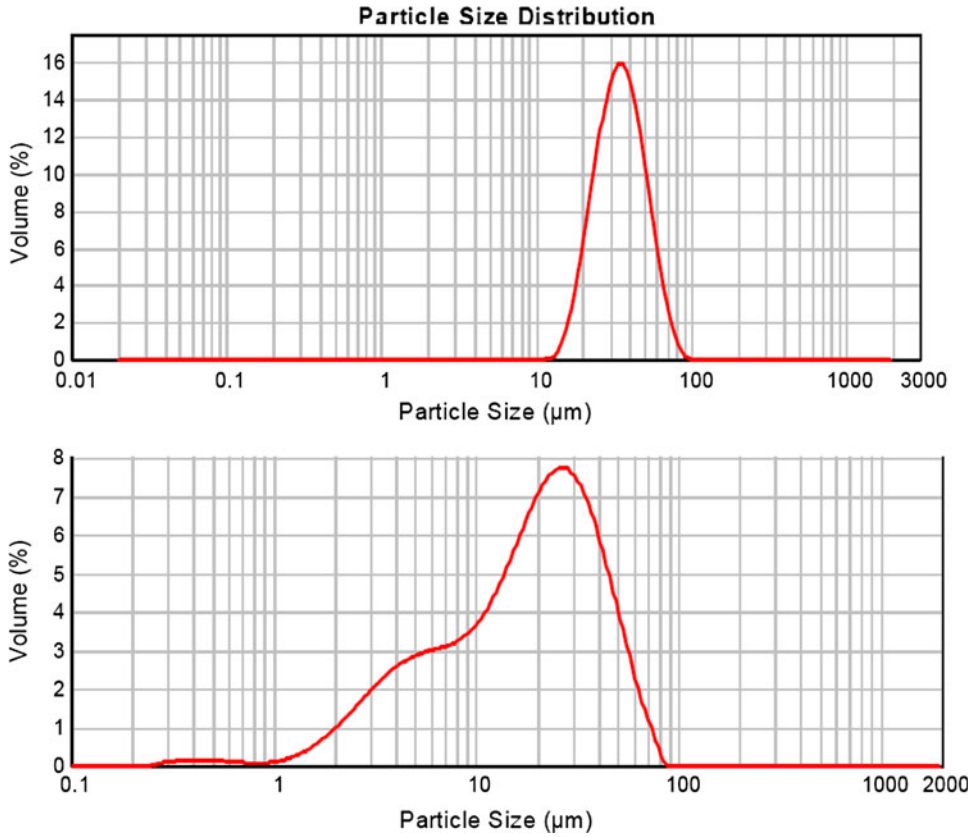

Fig. 1 Powders size distribution alumina (top) and YSZ (bottom)

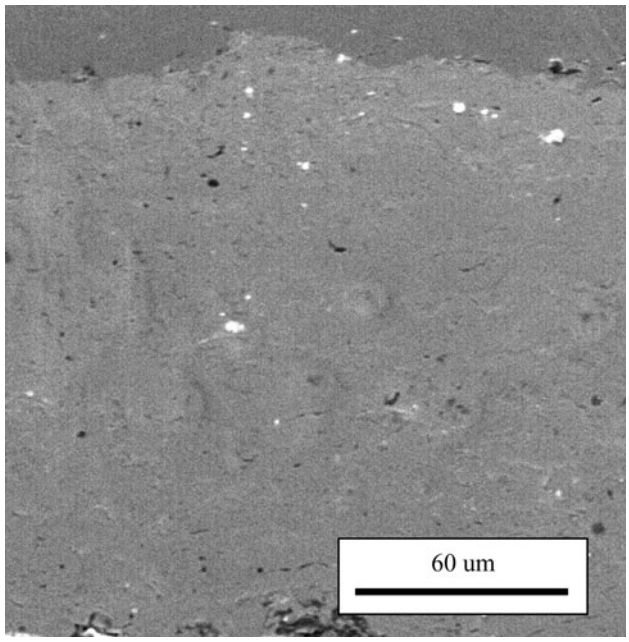

Fig. 2 Cross section of alumina coating

result in the curl-up of the edges of splats on the surface. Based on this assumption, Ghafouri et al. developed a mathematical model to calculate the angle of the curl-up

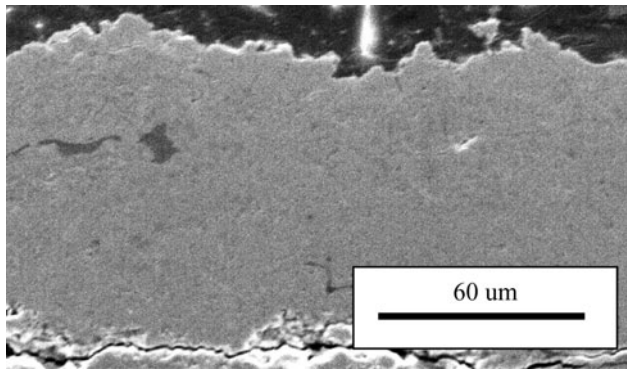

Fig. 3 Cross section of zirconia coating

based on the size of the splat and the thermal properties of the material, hence determining the void fraction that it would create. Although this assumption is very reasonable when depositing metal particles, in ceramic coatings where the residual stresses are relieved by the development of micro-cracks, there is no curl-up and formation of porosity related to other factors.

According to Xue et al. (Ref 4, 5) in ceramic coatings, porosity is formed because of the incomplete filling of the interstices on previously deposited splats, since surface tension prevents molten ceramic from entering small gaps. Xue et al. further developed and enhanced Ghafouri et al.

(Ref 1-3) model. As shown in Fig. 4, this model assumes that the impacting molten droplet is in contact with a series of uniform hemispherical asperities on the surface along the splat radius. In order to calculate the volume of the voids created between the hemispheres and the liquid layer, the equilibrium profile of the liquid meniscus are calculated using a method in which the total potential and surface energies of the system are minimized. Knowing the shape of the liquid meniscus and the profile of the asperity, one can use the geometrical expressions and then integrate the gap area over the total length of the splat to calculate the volume of the incompletely filled voids. The details about this method are presented in Ref 4, 5.

In addition to curl up and incomplete filling of interstices, a third phenomenon may result in the formation of porosity. The small, satellite droplets which are formed when droplets splash and are settled on the surface also promote the formation of porosity. Based on this assumption, the number of satellite droplets, their sizes, and locations are approximated using the theories presented by Xue et al. (Ref 5). These satellite droplets, in turn, create surface roughness and the incomplete filling of the coating layer will create more porosity.

Presently, *SimCoat* is equipped with several options to let the user investigate the effect of different parameters and mechanisms on coating thickness and porosity:

- The first important option is the ability of the code to use either statistical information for particle parameters, e.g., diameter, velocity, and temperature. We will refer to this option as the "statistical data." The second option is to directly use the raw DPV 2000 measurements. We will refer to this option as "DPV2000 data."
- There is the option to model a stationary gun or a moving torch, using appropriate operational parameters like torch velocity. The torch velocity can be constant or may have a sinusoidal form.
- The present powder material database has property values for five types of metals and oxides. There is the option to add user defined property databases.
- Besides calculating the porosity based on the incomplete filling of the interstices on the surface, the code has the ability to include the effect of splat curl up and/or the presence of satellite droplets on coating porosity and their effect on microstructure.

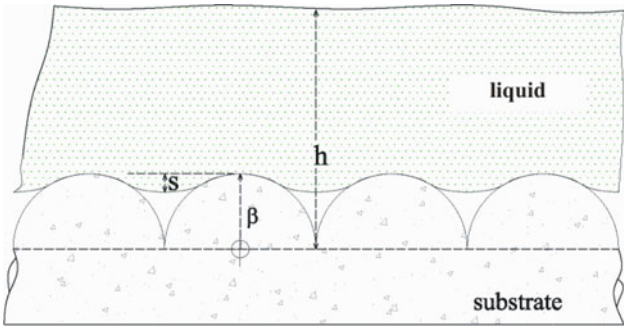

Fig. 4 Incomplete filling of the coating layer by new liquid material. The roughness on the solid surface is modeled as a series of hemispherical asperities located along the splat radius. *h* is the hydrostatic pressure of the new layer, β is the average size of the asperity, and *S* is the height of liquid, partially filled the gap between asperities

In this article, since we are considering only oxides (alumina and zirconia), splat curl-up is not an issue and this effect has not been considered. Also due to the high substrate temperature (400 °C), the probability of splashing and forming satellite droplets is minimal and thus, this option has also not been used.

Four sets of simulations were performed; two cases for the deposition of alumina coatings and two cases for zirconia. For each material, one simulation was performed using the statistical approach based on independent normal distribution of particle parameters. The statistical data were obtained by analyzing DPV-2000 measurements. In the second simulation, the raw DPV 2000 data which were recorded during the same measurement were used.

Table 2 lists the statistical information used for both simulations. As shown in Fig. 1, the actual mean particle diameters reported by the manufacturer are smaller than those recorded by DPV 2000. In the simulation, we have used the data provided by the manufacturer. The mean diameters and the corresponding standard deviations are shown in parenthesis in Table 2. Due to this difference, all particle diameters recorded by DPV 2000 which were directly used in simulations were corrected and calibrated with the manufacturer's data. As shown in Table 2, the mean temperature for zirconia is close to its melting point, indicating that the deposition efficiency may not be very high. However, for alumina this temperature is well above its melting point, which ensures significantly higher deposition efficiency (see Table 4 for melting point data). For alumina, the typical deposition efficiency reported by the plasma torch manufacturer is 50-70%.

Table 2 Average particles' diameter, velocity, and temperature obtained by DPV measurements for alumina and zirconia coatings

	Mean diameter	Standard deviation	Mean velocity	Standard deviation	Mean temperature	Standard deviation
Property	microns		m/s		°C	
Alumina	46 (37)	±20.44 (±10)	219	±55	2606	±225
Zirconia	66 (22)	±31.15 (±10)	404	±95	2657	±397

The numbers in the parenthesis are the actual numbers used in simulations. Please see the text

Table 3 Operating conditions

Experimental parameters	Alumina	Zirconia
Mass flow rate, g/s	0.43	0.666
Coating efficiency, %	80	30
Number of layers	10	13
Substrate size, mm	25 by 25	25 by 25
Substrate temperature, °C	400	400
Torch velocity (*X* direction), cm/s	63.5	63.5
Torch step size (*Y* direction), mm	5.6	5.6
Distance to substrate, mm	100	100
Spray dispersion angle, degrees	0 ± 20	0 ± 20

Table 4 Thermophysical properties of alumina and zirconia used in the present simulation

Property	Alumina	zirconia
Density, kg/m^3	3000 (Ref 6)	5600
Melting point, °C	2050	2690
Heat of fusion, J/kg	1.075E+6	0.78E+6
Kinematic viscosity at melting point, m^2/s	1.02E−5 (Ref 6)	5.1E−6 (Ref. 7)
Thermal conductivity at melting point (liquid & solid), W/m K	6	2
Specific heat at melting point (liquid-solid), J/kg K	1273-1300	962.8-830.7

The spray operating conditions used for both materials are listed in Table 3. There are a few important points that must be considered about the deposition conditions:

1. The deposition efficiency is a property that is difficult to measure during the coating process. Many parameters affect the deposition efficiency, including operating conditions of the torch and powder properties. As can be seen in Table 2, for Alumina coating, the efficiency must be rather high and most of the particles which arrive at the substrate are deposited. Thus for alumina, we assumed a deposition efficiency of 80%. However, for zirconia, the deposition efficiency must be lower and that is due to the fact that the average particle temperature is closer to the melting point of zirconia (see Table 2 and 4). The relatively low particle temperature indicates that many zirconia particles are either partially molten or not melted at all. It may be noted that the thermal conductivity of zirconia is rather low (1-2 W/m K) and many particles will not be completely melted during their flight toward the substrate and, possibly, they will bounce back from the surface. Therefore, for zirconia, we have assigned a deposition efficiency of only 30%, which is consistent with those reported in literature, e.g., Ref 8, 9.
2. The total number of gun passes, i.e., number of times that the gun moves from one side to the other side of the substrate on a straight line before it steps to the new location, can be obtained by multiplying the number of required coating layers by the number of passes that the gun must travel on the substrate to cover the whole surface. In this case, since the substrate has a width of 25 mm and the step size is 5.5 mm, it must travel five times to cover the whole substrate before it moves to the starting position. Therefore, for alumina coating, the total number of passes is 50 and for zirconia it is 65.
3. The spray dispersion angle can be obtained from the distance between the gun and the substrate and the diameter it can cover. The observations from the DPV 2000 measurement indicated that the spray distribution in this specific experiment was wide. In other words, by looking at the total number of particles spotted at different locations on the grid, we noticed the number of particles do not vary by much across the grid. For example for alumina, they number between 500 and 700 (see Fig. 5). This is an indication that a special form of the distribution function must be used to evaluate the possible number of droplets impinging on the substrate at different locations. Thus, to avoid concentration of the particles in the middle of the plume, we chose a larger standard deviation of 20 degrees. Usually this value is less than 10 degrees.

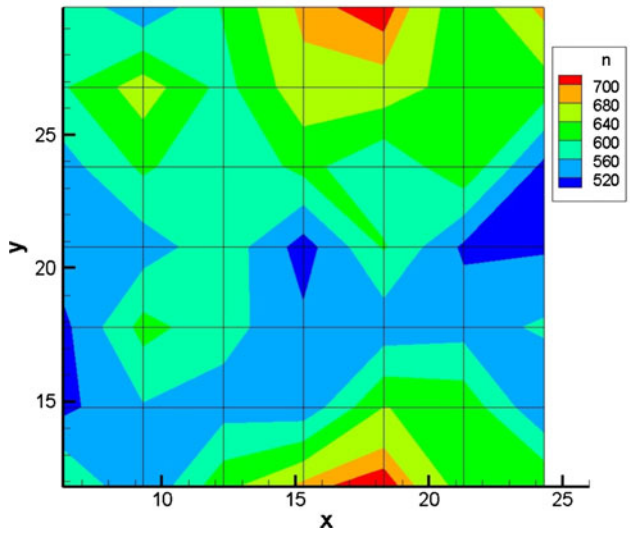

Fig. 5 Measured particle number density distribution for alumina powder at spray distance

The major properties of zirconia and alumina used in these simulations are presented in Table 4. In order to calculate the viscosity of liquid zirconia, we used Ref 7.

4. Results

4.1 Alumina—Statistical Data

In the first case, using the statistical data listed in Table 2, the coating formation of alumina on a stainless steel substrate was modeled. Upon termination of the simulation, the code generates two graphic files that show

Table 5 Simulation results, statistical information (Al_2O_3)

Parameter	Experiment	Simulations (statistical data) average	
		X direction	*Y* direction
Porosity, %	1-2	1.025	1.026
Thickness, μm	170-200	266	253
Roughness, μm	4.8-14	31.1	24.9

the isometric view of the coating layer and a cross section at the middle of the substrate perpendicular to the direction of the torch movement. The code also calculates the average porosity of the coating at two planes in the middle of the substrate, one parallel and one perpendicular to the gun movement. The coating thickness and surface roughness are also calculated at these two planes. A summary of the simulation results is presented in Table 5. Also in this table are the corresponding values obtained from the measurements that are shown for comparison.

The predicted porosity values agree reasonably well with the measured ones. However, the coating thickness is over-estimated by the model. One parameter that affects this prediction is the deposition efficiency which is an input to the model. If this is over-estimated, then the coating thickness will also be over-estimated. This appears to be the case here. The discrepancy between the predicted and measured roughness will be discussed later in the article.

Figure 6 shows an isometric view of the coating. Different colors indicate the height of the coating, red being the thickest and blue the thinnest part. One feature of this figure is the existence of ribbons of thicker coatings. These ribbons are formed right underneath the torch and in the direction of its movement. The reason for this is that the particle dispersion angle assumes a Gaussian shape, meaning most of the particles are thereby released in the central core of the plume and hills are formed as a result. Note that the distance between these ribbons is the same as the gun step size. It must be noted that in practice, the initial position of the torch after covering one layer of the coating on the surface will be changed and therefore, these ribbons of high level coating will not be formed. However, in this set of experiments and simulations, the starting location of the gun remained the same, causing formation of these ribbons of thicker coating.

Another feature of the predicted coatings is that the coating is thinner at the edges of the substrate. This is based solely because in these simulations where we assumed that the gun starts to move just from the edge of the sample and stops at the other edge. Therefore, because of the dispersion angle, the number of particles that are deposited at the edges are smaller than the rest of the substrate. This means that the coating becomes thinner at the edge of the sample.

Figure 7 shows a cross section of the coating shown in Fig. 6 at the middle of the substrate and perpendicular to the torch movement. The "*z*" axis in this figure is not to

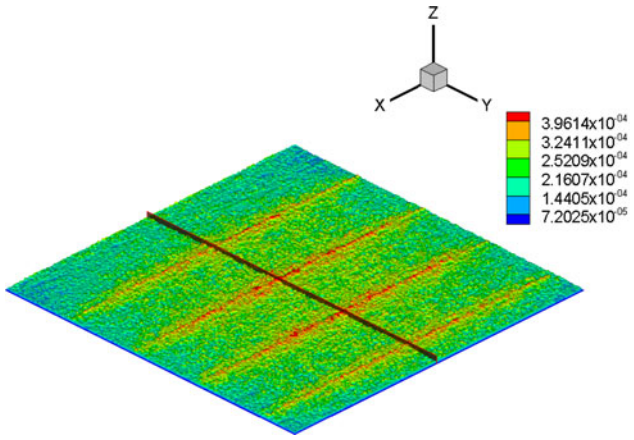

Fig. 6 Isometric view of alumina coating, using the statistical data for the particles. The legend shows the thickness of the coating in (m)

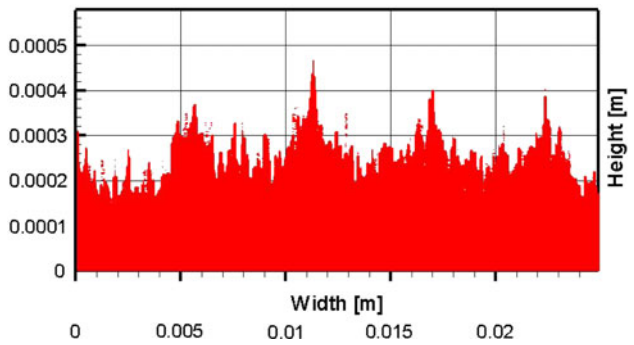

Fig. 7 Cross section of the coating along the plane shown in Fig. 6

scale so one can clearly observe the roughness of the surface as well as porosity. Please note that since the porosity is very small (1-2%) in this case, it is not very visible in the figure.

To calculate the surface roughness, first the local average thickness of the coating at a selected cross section is calculated by fitting a spline. The roughness is then calculated by averaging the absolute value of the difference between the actual local thickness and the average local thickness. Due to the existence of the thick ribbons, the average roughness in the "*X*" direction is higher than in the "*Y*" direction (see Table 5 and Fig. 6).

4.2 Alumina—DPV 2000 Data

In this part we present the results of the simulations which were performed using the DPV 2000 measurement results for particles' diameter, velocity, and temperature. The variation of particle conditions through the cross section of the plasma plume was collected by 7 by 7 grid scans at 3 mm steps at 100 mm spray distance, in the absence of a substrate. The collected data is recorded in the form of the location of the particles' diameter, velocity, and temperature. At each specific location, as low as

one particle to tens of particles may be detected and the corresponding properties are recorded. Since the distance between the torch tip and the plane at which the information is recorded by DPV is the same as the gun and the substrate, it can be assumed that the particle velocity and temperatures measured by DPV are the same as those impacting the substrate.

In *SimCoat* software, the option is provided to read the data collected by DPV 2000. If this option is selected, the information on each particle (location, diameter, velocity, and temperature) is read from the DPV 2000 output file. The substrate is then divided into 3 by 3 mm^2 zones (grids) and all particles passing through a specific grid are listed in a table based on their diameters. For each particle size, a velocity and a temperature would be recorded. It is possible that at each grid, there is more than one particle with the same diameter. However, particles of the same size may have different temperature and/or velocity. All this information is tabulated in a format that is searchable by the software.

At each gun movement when executing *SimCoat*, a series of particles are released from the gun. The number of particles is determined based on an average particle size, feed rate, and deposition efficiency. The landing location for each particle is determined using the dispersion angle and the gun distance from the substrate. The dispersion angle is statistically determined from its average and its standard deviation values.

For each particle landing on the surface, first the landing position is obtained as described above. Then based on the position of torch center line at that specific time, the location of the particle in the DPV2000 scanning grid is determined.* Knowing the particle position in the grid, the database of *SimCoat* that contains the measurements information of DPV2000 is searched and corresponding particles and their properties at the same vicinity are determined:

- If there is only one particle detected in that location by DPV, the corresponding diameter, temperature, and velocity is selected and used in the simulation.
- If there are more than one particle detected at that grid (which is usually the case) the following actions are taken:
  - First using a random number generator routine, one particle size is selected from the list.
  - If for that particle size, only one temperature and velocity are measured, those values are selected.
  - If more than one temperature and/or velocity is recorded, using the random number generator once more, one pair is selected and the information is used as the initial condition for that particle.

*The particle conditions at specific locations on the scanning grid are measured by DPV2000. During these measurements, the position of the torch is fixed during plasma coating operation; however, plasma torch is moving and is not stationary. Therefore, at each time step, the measured particles' positions by DPV2000 are adjusted to correspond to the new position of the plasma gun and the center of the scanning grid.

Table 6 Simulation results using DPV information (Al_2O_3)

		Simulations (DPV) average	
Parameter	**Experiment**	***X* direction**	***Y* direction**
Porosity, %	1-2	1.4	1.36
Thickness, μm	170-200	137	118
Roughness, μm	4.8-14	22	13.2

Table 7 Simulation results, statistical information (YSZ)

		Simulations (statistical data) average	
Parameter	**Experiment**	***X* direction**	***Y* direction**
Porosity, %	1-2	1.92	1.94
Thickness, μm	70	149.6	137.4
Roughness, μm	7-14.9	18	15

In this case, we use the direct DPV measurement results which are of course the same as the actual spraying conditions. For example, DPV results show that the particle stream is usually less dense around the periphery of the jet and the particles are much hotter in the center of the Axial III plasma jet.

Table 6 shows the summary of simulation results for alumina using the direct DPV measurements. As can be seen, in this case the predicted coating thickness is less than the one by statistical model obtained under the same conditions. Also the roughness results have improved and are closer to the measured values.

4.3 Zirconia—Statistical Data

Simulations were repeated for zirconia powders under the conditions reported in Table 3. Table 7 shows the simulation results using the statistical information of Table 2 and the corresponding experimental data.

Due to the high-particle velocity and temperatures, the porosity values obtained for zirconia both from experimental observation and simulation are relatively low. Also, similar to the results obtained for alumina, the roughness is higher in the "*X*" direction than the "*Y*" direction.

Figure 8 shows the isometric view of the zirconia coating, for a 25 by 25 mm^2 substrate. As was the case for alumina, the same ribbons of thicker coatings are observed. Again, the torch moves exactly from one side of the substrate to the other side, resulting in higher coating thickness at the middle of the substrate. A close up image of the coating is inserted in this figure, showing the surface roughness in detail (the figure is not to scale). Figure 9 shows the cross section of the same coating, taken at the location shown in Fig. 8.

4.4 Zirconia—DPV data

Simulations were performed for zirconia using the DPV 2000 data as described in Section 4.2. Due to the higher

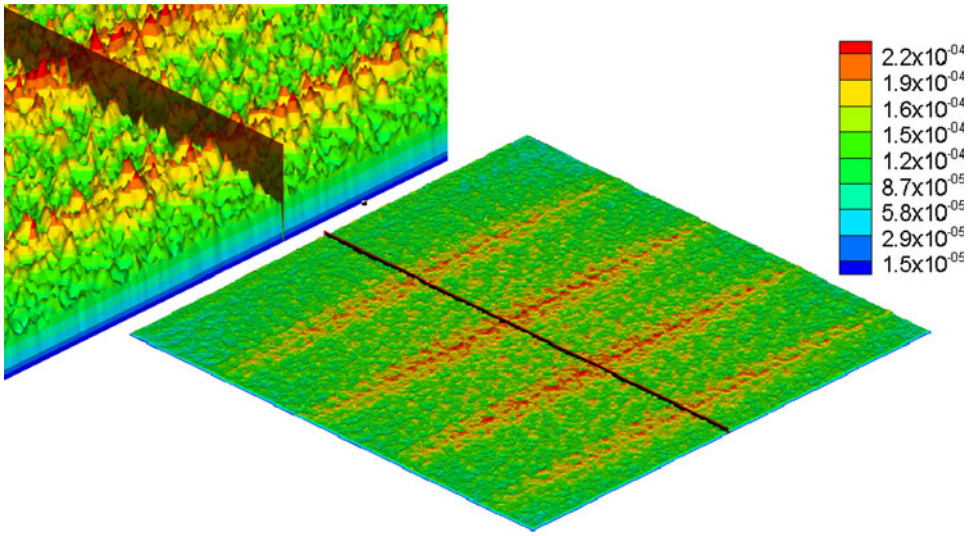

Fig. 8 Isometric view of zirconia coating on the surface, using statistical data. Inset shows a close up of the coating, simulated by the code

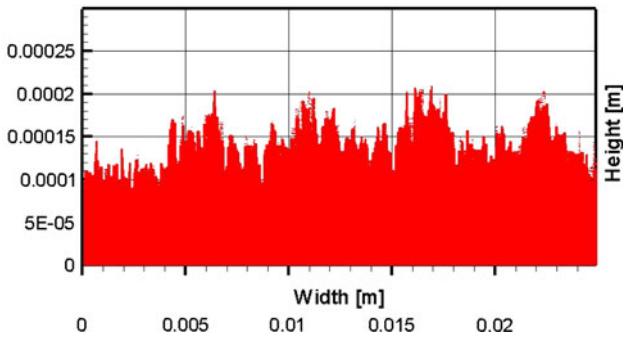

Fig. 9 Cross section of the coating at the location shown in Fig. 8

number of passes and larger flow rate of particles, and the fact that the code needs to search the particle data base to find the matching velocity and temperature for each particle, the memory demand for running the simulations on a 25 by 25 mm surface and 13 layer of coating (60 passes) was so high that our system (2 GB RAM) could not continue the simulations. This problem will be eliminated by using a 64 bit system which can utilize larger memories (6-8 GB). Therefore, to save both CPU time and memory, we reduced the size of the substrate to 6 by 25 mm.

Table 8 summarizes the simulation results for zirconia using DPV data. The simulation results are closer to the experimental measurements when the actual particle information is used. It may be noted that in this case, the average coating roughness is also very close to the measured values.

5. Discussions

As it was shown in previous sections, *SimCoat* is able to predict the coating thickness and porosity with a good degree of accuracy. Especially, we showed that when DPV 2000 measurements are used as input to the code, the simulation results for coating thickness are closer to the measured data.

Table 8 Simulation results (YSZ), DPV

		Simulations (DPV) average	
Parameter	**Experiment**	***X* direction**	***Y* direction**
Porosity, %	1-2	1.43	1.37
Thickness, μm	70	71.4	63.8
Roughness, μm	7-14.9	10.7	8.6

Because of the higher temperature and the higher speed of the sprayed particles associated with Axial III spray torch, the coatings are very dense (Fig. 2, 3). Our simulations also showed that the porosity of the coatings for both zirconia and alumina are very low which is in agreement with the measurement. Please note that the location and the size of the samples that were cut and used for measuring the thickness, roughness, and porosity of the coatings were not exactly known. Therefore, a direct comparison is not possible. Because there were ribbons of thicker coatings (Fig. 6, 8) on the surface, the average calculated values of roughness do not match very well with the experimental data.

The simulation showed that the software is able to simulate the larger sample sizes (in this study 25 by 25 mm^2) with a larger number of coating layers, within a reasonable time. Our simulations were completed in less than 3 h (for zirconia coating on the small substrate) to about 24 h (for alumina coating using DPV data). This is a very important improvement to the earlier model, since the calculated results will be more representative of the actual coatings. The model can be used to investigate the effect of physical properties of materials, like viscosity and density, as well as spraying parameters

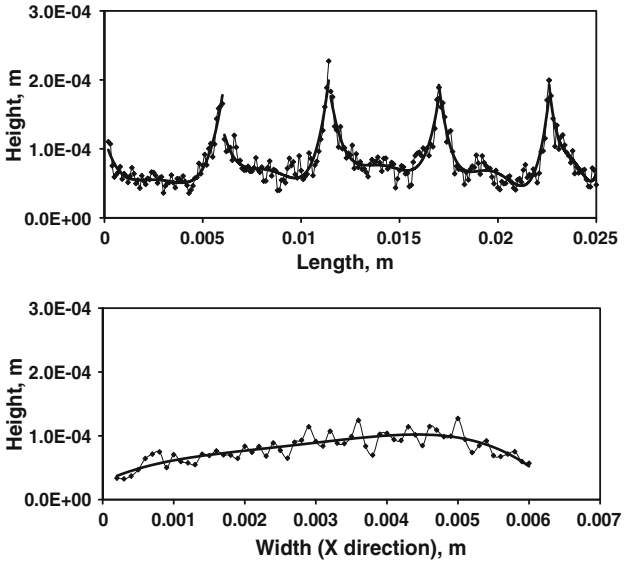

Fig. 10 Surface roughness analysis. *Top*: Surface height at different locations along the "*y*" axis taken at the mid surface of the coating layer (for example see Fig. 6). *Bottom*: Surface height at different locations along the "*x*" axis. A regression analysis of the data in Excel was used to generate the average height of the coating layer. The average roughness was then calculated based on the average height of the layer

like particles' velocity and temperature, on the coating quality.

To calculate the average surface roughness, a spline is fitted through a cross section (Fig. 10). The fit represents the average thickness of the coating. The average roughness is then calculated by calculating the absolute difference between the average and local thickness of the coating at every location and averaging it over the cross section.

The difference between the calculated thickness and the experimental measurement is due to a number of factors. First, we do not have a good estimate of the deposition efficiency and we must use the values suggested either by the plasma torch and/or powder manufacturers or rely on values reported in the literature. Second, we have showed that, compared to the statistical method, using DPV 2000 measured values as input results in a better estimate of the thickness. Results of such measurements may not, however, be readily available.

The present code does not calculate the surface area of the cracks. However, in order to determine the residual stress and the shrinkage of the coating microstructure, the simulation results can be used as input to OOF software (Ref 10), a finite element algorithm for calculating residual stresses in the coating, developed by National Institute for Standards and Technologies (NIST). More details describing the process are presented in Ref 2, 10, 11.

6. Conclusions

This article presents a computational approach to modeling formation of thermal spray coatings and prediction of their microstructure as a function of the impact conditions of the injected powders. Two types of ceramic coatings were considered, i.e., alumina and yttria-stabilized zirconia. Predictions of the model were compared with the actual coatings deposited under the same conditions. One unique feature of this model is that it is able to use the actual measured impact conditions provided by the widely used DPV 2000. The other option is to describe the distribution of the impact parameters, including their average value and standard deviation, and predict the microstructure. We found that providing DPV 2000 data results in a more accurate estimate of the coating properties, e.g., average roughness, etc. Another important feature of the model is that it is now possible to model large substrate sizes, e.g., 25 by 25 mm. Due to the computational time, previously reported models were limited to much smaller substrate sizes.

In summary, this model could be an excellent tool in developing new coatings and parametrically studying how different impact parameters can affect microstructure.

References

1. R. Ghafouri-Azar, J. Mostaghimi, S. Chandra, and M. Charmchi, A Stochastic Model to Simulate the Formation of Thermal Spray Coating, *J. Thermal Spray Technol.*, 2003, **12**(1), p 53-69
2. R. Ghafouri-Azar, J. Mostaghimi, and S. Chandra, Modeling Development of Residual Stresses in Thermal Spray Coatings, *Comput. Mater. Sci.*, 2006, **35**, p 13-26
3. R. Ghafouri-Azar, S. Shakeri, S. Chandra, and J. Mostaghimi, Numerical Simulation of Offset Deposition for Sequential Tin Droplet, *Proceeding of International Thermal Spray Conference and Exposition*, March 4-6, 2002 (Germany), 2002, p 951-959
4. M. Xue, S. Chandra, and J. Mostaghimi, Investigation of Splat Curling Up in Thermal Spray Coatings, *J. Thermal Spray Technol.*, 2006, **15**(4), p 531-536
5. M. Xue, S. Chandra, J. Mostaghimi, and C. Moreau, A Stochastic Coating Model to Predict the Microstructure of Plasma Sprayed Zirconia Coatings, *Modell. Simul. Mater. Sci. Eng.*, 2008, **16**(6), p 19
6. Y. Kawai and Y. Shiraishi, *Handbook of Physico-Chemical Properties at High temperatures*, Iron and Steel Institute of Japan, 1988, p xxi
7. K. Shinoda, Y. Kojima, and T. Yoshida, In Situ Measurement System for Deformation and Solidification Phenomena of Yttria-Stabilized Zirconia Droplets Impinging on Quartz Glass Substrate Under Plasma Spraying Conditions, *J. Thermal Spray Technol.*, 2005, **14**(4), p 511-517
8. G. Mauer, R. Vaßen, and D. Stövre, Atmospheric Plasma Spraying of Yttria-Stabilized Zirconia Coating with Specific Porosity, *Surf. Coat. Technol.*, 2009, **204**, p 172-179
9. H. Chen, S.W. Lee, H. Du, C.X. Ding, and C.H. Choi, Influence of Feedstock and Spraying Parameters on the Depositing Efficiency and Microhardness of Plasma-Sprayed Zirconia Coating, *Mater. Lett.*, 2004, **58**, p 1241-1245
10. OOF: Finite Element Modeling for Materials Science, NIST, http://www.nist.gov/msel/ctcms/oof/
11. J. Mostaghimi, S. Chandra, R. Ghafouri-Azar, and A. Dolatabadi, Modeling Thermal Spray Coating Processes: A Powerful Tool in Design and Optimization, *Surf. Coat. Technol.*, 2003, **163-164**, p 1-11